RSC Medicinal Chemistry

ROYAL SOCIETY OF CHEMISTRY

RESEARCH ARTICLE

Cite this: *RSC Med. Chem.*, 2021, **12**, 1910

Synthesis and antitumour evaluation of indole-2-carboxamides against paediatric brain cancer cells†

Shahinda S. R. Alsayed,[a] Amreena Suri,[b] Anders W. Bailey,[b] Samuel Lane,[c] Eryn L. Werry,[cd] Chiang-Ching Huang,[e] Li-Fang Yu,[f] Michael Kassiou,*[c] Simone Treiger Sredni*[bg] and Hendra Gunosewoyo*[a]

Paediatric glioblastomas are rapidly growing, devastating brain neoplasms with an invasive phenotype. Radiotherapy and chemotherapy, which are the current therapeutic adjuvant to surgical resection, are still associated with various toxicity profiles and only marginally improve the course of the disease and life expectancy. A considerable body of evidence supports the antitumour and apoptotic effects of certain cannabinoids, such as WIN55,212-2, against a wide spectrum of cancer cells, including gliomas. In fact, we previously highlighted the potent cytotoxic activity of the cannabinoid ligand **5** against glioblastoma KNS42 cells. Taken together, in this study, we designed, synthesised, and evaluated several indoles and indole bioisosteres for their antitumour activities. Compounds **8a**, **8c**, **8f**, **12c**, and **24d** demonstrated significant inhibitory activities against the viability (IC_{50} = 2.34–9.06 μM) and proliferation (IC_{50} = 2.88–9.85 μM) of paediatric glioblastoma KNS42 cells. All five compounds further retained their antitumour activities against two atypical teratoid/rhabdoid tumour (AT/RT) cell lines. When tested against a medulloblastoma DAOY cell line, only **8c**, **8f**, **12c**, and **24d** maintained their viability inhibitory activities. The viability assay against non-neoplastic human fibroblast HFF1 cells suggested that compounds **8a**, **8c**, **8f**, and **12c** act selectively towards the panel of paediatric brain tumour cells. In contrast, compound **24d** and WIN55,212-2 were highly toxic toward HFF1 cells. Due to their structural resemblance to known cannabimimetics, the most potent compounds were tested in cannabinoid 1 and 2 receptor (CB_1R and CB_2R) functional assays. Compounds **8a**, **8c**, and **12c** failed to activate or antagonise both CB_1R and CB_2R, whereas compounds **8f** and **24d** antagonised CB_1R and CB_2R, respectively. We also performed a transcriptional analysis on KNS42 cells treated with our prototype compound **8a** and highlighted a set of seven genes that were significantly downregulated. The expression levels of these genes were previously shown to be positively correlated with tumour growth and progression, indicating their implication in the antitumour activity of **8a**. Overall, the drug-like and selective antitumour profiles of indole-2-carboxamides **8a**, **8c**, **8f**, and **12c** substantiate the versatility of the indole scaffold in cancer drug discovery.

Received 26th February 2021,
Accepted 5th August 2021

DOI: 10.1039/d1md00065a

rsc.li/medchem

1. Introduction

Gliomas are brain tumours that originate from non-neuronal supportive cells, called glial cells, which are the most abundant cell types in the central nervous system (CNS).[1,2] Paediatric gliomas represent the most common CNS tumours and the leading cause of cancer-related death in children. The average annual incidence rate of CNS tumours in children (0–14 years old) is 5.26 per 100 000 with gliomas accounting for approximately 53% of tumours in this age cohort.[3] Gliomas are classified based on the histological criteria of neoplasms into a grading system of malignancy by the World Health Organisation (WHO). The three main categories of gliomas are low grade gliomas (LGGs, WHO grade I and II), high grade gliomas (HGGs, WHO grade III

[a] *Curtin Medical School, Faculty of Health Sciences, Curtin University, Bentley, Perth, WA 6102, Australia. E-mail: Hendra.Gunosewoyo@curtin.edu.au*
[b] *Division of Pediatric Neurosurgery, Ann and Robert H. Lurie Children's Hospital of Chicago, Chicago, IL 60611, USA. E-mail: simone.sredni@gmail.com*
[c] *School of Chemistry, The University of Sydney, NSW, 2006, Australia. E-mail: michael.kassiou@sydney.edu.au*
[d] *Faculty of Medicine and Health, The University of Sydney, NSW 2006, Australia*
[e] *Department of Biostatistics, Zilber School of Public Health, University of Wisconsin, Milwaukee, WI 53205, USA*
[f] *Shanghai Engineering Research Center of Molecular Therapeutics and New Drug Development, School of Chemistry and Molecular Engineering, East China Normal University, 3663 North Zhongshan Road, Shanghai 200062, China*
[g] *Department of Surgery, Northwestern University, Feinberg School of Medicine, Chicago, IL 60611, USA*

† Electronic supplementary information (ESI) available. See DOI: 10.1039/d1md00065a

and IV) and diffuse midline gliomas (DMGs).[4] These three tumour entities require different treatment and/or management strategies. Paediatric HGGs are nearly universally fatal brain tumours associated with dismal prognosis, with a median survival of 1–2 years.[5] A key element hampering the development of new targeted therapies is the relative shortage of paediatric glioma cell lines.[6] Despite the clear histopathological similarities between HGGs of all ages, the well-established commonly used adult cell lines are not truly representative of the distinct molecular signatures of childhood HGGs.[6–8] Hence, there is a pressing need to develop novel therapeutic agents that effectively target paediatric brain tumours.

We are particularly interested in paediatric glioblastoma multiforme (GBM or grade IV astrocytoma) which is among the most malignant, aggressive and invasive CNS tumours in children.[3] The mainstays of treatment of GBM are only palliative, including surgical resection when applicable followed by focal radiotherapy combined with chemotherapy. Many chemotherapeutic agents have been tested including temozolomide, but no remarkable improvement on survival has been achieved in paediatric GBM.[5,9] The druggable molecular targets in paediatric HGGs and their corresponding drug candidates that are currently in clinical trials have been recently reviewed.[10] In the adult GBM counterpart, Guzman *et al.* first reported their pilot phase I clinical trial findings on the efficacy of the phytocannabinoid derivative Δ^9-tetrahydrocannabinol (Δ^9-THC, **1**, Fig. 1) delivered intracranially to nine patients.[11] This cannabinoid was found to be fairly safe (no overt psychoactive effects) and inhibited tumour cell proliferation in a subset of patients.[11]

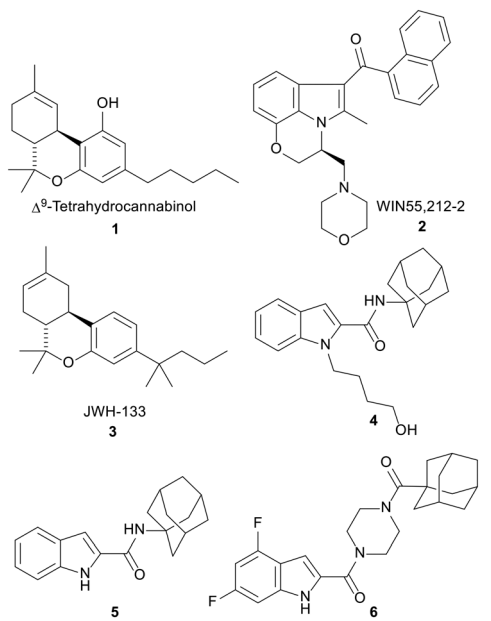

Fig. 1 CB ligands **1**–**5** as well as the antitumour indoleamide analogue **6** which was identified in our previous report. Δ^9-Tetrahydrocannabinol (**1**) and WIN55,212-2 (**2**) are mixed CB_1R/CB_2R agonists, while compounds **3**–**5** are selective CB_2R agonists.

In fact, since the *in vitro* antitumour potential of Δ^9-THC was first reported in 1975,[12] an accumulating body of research has demonstrated the antineoplastic effects of many endogenous, naturally occurring, and synthetic cannabinoids against various tumour cells, including gliomas.[13–20] These compounds produce most of their biological effects by targeting cannabinoid 1 and 2 receptors (CB_1R and CB_2R) which are present in the brain and the periphery.[21] In particular, two mixed CB_1R and CB_2R agonists, Δ^9-THC (**1**) and WIN55,212-2 (**2**), in addition to the selective CB_2R agonist JWH-133 (**3**), Fig. 1, were shown to inhibit the growth of malignant gliomas and impair tumour angiogenesis *in vitro* and in animal models. They also induced apoptosis in glioma cells *in vitro* and tumour regression *in vivo*.[22–28] A number of reports ascribed the antitumour activities of cannabinoids to the CB receptors, whilst others demonstrated that their antitumour activities are independent of CB receptors.[24–26,29–36] Hence, the mechanism of action of cannabinoids as antitumour agents is still debatable.

In light of the widely reported antitumour activities of cannabinoids, we were interested in exploring the structure–antitumour activity relationship of the indole-containing cannabimimetic agents, exemplified by WIN55,212-2. Indeed, we previously reported several indolecarboxamide derivatives as potent CB_1R and/or CB_2R ligands.[37] The potent CB_2R agonist *N*-(1-adamantyl)-1-(4-hydroxybutyl)-indole-2-carboxamide (**4**) was the highlight of our previous work (CB_2R EC_{50} = 0.12 μM) which showed no agonist or antagonist activity at CB_1R. We also found in the same report that the *N*-unsubstituted indole **5** exhibited a similar selective CB_2R functional activity (EC_{50} = 0.98 μM) to the *N*-alkylated indole **4**.[37] Importantly, we demonstrated the potent inhibitory activity of compound **5** against the viability of paediatric GBM KNS42 cells (IC_{50} = 0.33 μM).[38] In this report, we brought to light the cytotoxic and antiproliferative activities of the indole-2-carboxamide **6** against different malignant brain tumour cells.

Accordingly, in the current study, we describe the design, synthesis, and biological evaluation of several *N*-unsubstituted indoles and indole bioisosteres as antitumour agents. All final analogues as well as reference ligands WIN55,212-2, JWH-133, and compound **4** were screened *in vitro* for their viability and proliferation inhibitory activities against paediatric GBM KNS42 cells. KNS42 was the cell line of choice in our primary antitumour screening as it is reported to overexpress CB_1R (encoded by the *CNR1* gene).[39] The antitumour and safety profiles of the most potent compounds were then scrutinised in non-GBM high-grade paediatric brain tumour cells [teratoid/rhabdoid AT/RT (BT12 and BT16) and medulloblastoma (DAOY)] as well as non-neoplastic HFF1 cells. In addition, the functional activities of the top active compounds at CB_1R and CB_2R were assessed and a transcriptional analysis of KNS42 cells treated with the *N*-benzylindoleamide analogue **8a** was conducted. The drug-likeness of the most active compounds was also predicted using ACD/Labs Percepta.

2. Design

In compounds **8a–f**, a 4,6-difluoro-1*H*-indole nucleus was used instead of the unsubstituted-1*H*-indole in compound **5**, while the adamantane ring was replaced with benzyl, piperonyl, and homopiperonyl motifs. The 4,6-difuoroindole was the scaffold of choice in our study as it has higher lipophilicity (Clog*P* = 2.6) compared to the unsubstituted indole ring (Clog*P* = 2.1). In this respect, the slight increase in lipophilicity of the 4,6-difluoroindole-containing compounds may enhance their uptake by tumour cells[40] which can lead to an improved antitumour activity profile without significantly impacting the drug-like properties. We also probed the activity of the benzimidazole and indazole cores as bioisosteric replacements to the indole moiety while retaining the adamantane appendage in compounds **10**, **12a–c**, and **14**. In a different approach, we also investigated the activity of some adamantane-derived indoles, wherein extra spacers were introduced to the amide linker between the 4,6-difluoroindole core and the adamantane ring, forming the diamides **18** and **23a** and **b**. It is noteworthy that compound **23a** was previously evaluated in our recent report[38] and is reincorporated herein to be compared to compound **23b**.

On the other hand, *N*-(1-adamantyl)-1-alkylquinolone-3-carboxamides were widely reported in the literature as cannabinoid receptor modulators.[41–44] In addition, some quinolone-3-carboxamides with selective CB_2R affinity previously showed potent reduction of the viability of the LNCaP prostatic cancer cell line, displaying IC_{50} values significantly lower than that of JWH-133 (**3**).[45] Accordingly, in line with the aforementioned strategies, we tested several *N*-unsubstitutedquinolone-3-carboxamides **24a–e** and their analogous quinolone-2-carboxamide counterparts **25a–e** for their antitumour activities. Of note, all of the tested quinolonecarboxamides **24a–e** and **25a–e** were previously evaluated for their antitubercular activity, whereupon most of them were found to be inactive.[46]

3. Chemistry

The synthetic strategies of all the final compounds are depicted in Schemes 1 and 2. Reference cannabimimetic indoles **4** and **5** were synthesised according to the reported procedure.[37] Indoles **8a–f**, benzimidazoles **10** and **12a–c**, and indazole derivative **14** were synthesised in a one-step amide coupling reaction (method A or B). The indole-2-carboxamides **8a–f** and benzimidazole-2-carboxamide **10** were obtained *via* reacting the carboxylic acid derivatives **7** and **9**, respectively, with the corresponding amines in the presence of 1-ethyl-3-(3-dimethylaminopropyl)carbodiimide hydrochloride (EDC·HCl), hydroxybenzotriazole hydrate (HOBt) and *N*,*N*-diisopropylethylamine (DIPEA) (method A). Method B [EDC·HCl and 4-dimethylaminopyridine (DMAP)] was conducted between compound **11** and the corresponding carboxylic acids to generate the benzimidazole derivatives **12a–c**. The indazole-3-carboxamide derivative **14** was formed

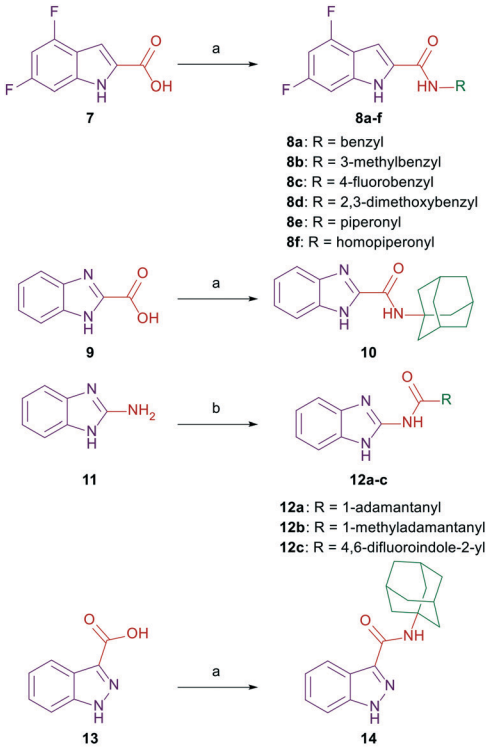

Scheme 1 General synthetic approach for compounds **8a–f**, **10**, **12a–c**, and **14**.

following the amide coupling protocol A between compound **13** and 1-adamantylamine (Scheme 1).

On the other hand, the synthesis of the adamantane-derived indole dicarboxamide derivatives **18** and **23a** and **b** is illustrated in Scheme 2. Compound **18** was prepared in three steps starting from coupling 1-adamantylamine (**15**) with *N*-(*tert*-butoxycarbonyl)glycine (Boc-Gly-OH) following a reported procedure[47] to give the *N*-(Boc) adamantane derivative **16**. Cleavage of the Boc group thereof using trifluoroacetic acid (TFA) yielded the aminoacetamide intermediate **17**. Employing method A of amide coupling, compound **17** was reacted with 4,6-difluoroindole-2-carboxylic acid (**7**) to afford the final compound **18**. Similar to our previously reported compound **23a**,[38] the dicarboxamide analogue **23b** was obtained in a four-step pathway starting from the initial protection of the amino group in the aniline **19b** using di-*tert*-butyl dicarbonate $(Boc)_2O$. Thereafter, the *N*-Boc derivative **20b** was subjected to amide coupling (method A) with 1-adamantylamine to provide compound **21b**. Subsequent *N*-Boc deprotection of the crude product **21b** under acidic conditions furnished the key intermediate **22b**. Finally, amide coupling of **22b** with **7** (method A) delivered the desired dicarboxamide analogue **23b** (Scheme 2). Compounds **24a–e** and **25a–e** were synthesised as reported in our previous work.[46]

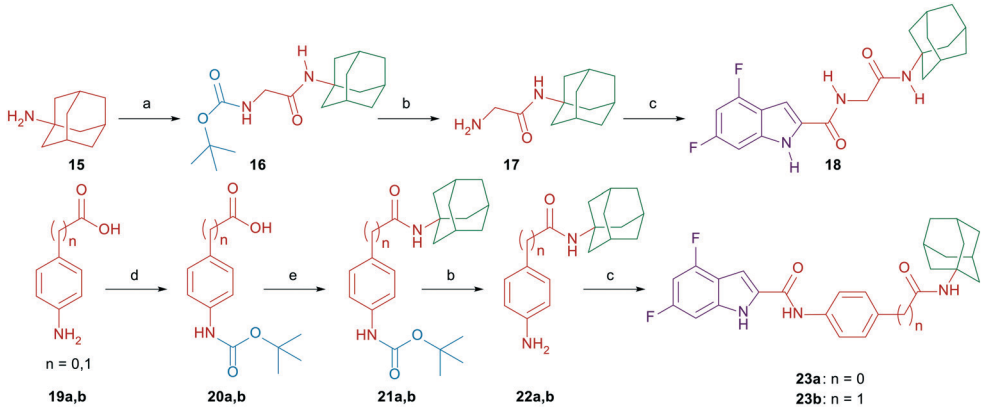

Reagents and conditions:
a) Boc-Gly-OH, EDC.HCl, DMAP, THF, DCM, rt, 72 h, 80%; b) TFA, DCM, rt, 12 h, 90-96%; c) EDC.HCl, HOBt, 4,6-difluoroindole-2-carboxylic acid, DIPEA, DMF, rt, 72 h, 25-96%; d) di-*tert*-butyl dicarbonate, triethylamine, dioxane, H_2O, rt, 72 h, 84-86%; e) EDC.HCl, HOBt, 1-adamantylamine, DIPEA, DMF, rt, 72 h, 70-84%.

Scheme 2 General synthetic approach for compounds **18** and **23a and b**.

4. Results and discussion

4.1. Biological evaluation and SAR analysis

4.1.1. Cytotoxicity and antiproliferative activity against paediatric KNS42 GBM cells. All the synthesised final compounds **8a–f**, **10**, **12a–c**, **14**, **18**, **23a and b**, **24a–e**, and **25a–e** were evaluated for their viability inhibition and antiproliferative activities against paediatric GBM KNS42 cells (Table 1). CB receptor ligands WIN55,212-2 (**2**), JWH-133 (**3**), **4**, and **5** were used as positive controls. Of note, WIN55,212-2 is a non-selective CB_1R/CB_2R agonist (CB_1R EC_{50} = 0.284 μM, CB_2R EC_{50} = 0.062 μM), whereas JWH-133 (CB_2R K_i = 0.0034 μM) and compounds **4** and **5** are selective CB_2R agonists (CB_2R EC_{50} = 0.12 and 0.98 μM, respectively).[37,48,49] Reference compounds **2**, **4**, and **5** showed moderate to high cytotoxic activities with low micro- and sub-micromolar inhibitory activities on cell viability (IC_{50} = 8.02, 4.75, and 0.33 μM, respectively). The selective CB_2R agonist JWH-133 (**3**) showed no inhibitory activity at 10 μM concentration against KNS42 cells in both viability and proliferation studies. WIN55,212-2 was the only active control that inhibited the proliferation of KNS42 cells (IC_{50} = 8.07 μM). The cytotoxic effects of selective CB_2R agonists **4** and **5** *versus* the inactivity of JWH-133 towards KNS42 cells suggest that these compounds may be impacting the cell viability of KNS42 cells *via* a CB receptor-independent mechanism. This notion is reinforced with many previous reports excluding the involvement of CB receptors in the antiproliferative and apoptotic effects of numerous cannabinoids.[22,26,31–36,50]

The first round of our investigations was focused on exploring the antitumour activity of the 4,6-difluoroindoleamides **8a–f**, benzimidazoleamides **10** and **12a–c**, and indazoleamide **14**. The *N*-benzyl-indoleamide analogue **8a** was previously evaluated in our recently published report.[38] It displayed an activity profile similar to WIN55,212-2 against KNS42 cells [IC_{50} (viability and proliferation) = 8.25 and 9.85 μM, respectively]. We then probed the effect of incorporating different substituents on the benzyl group in **8a** on the antitumour activity. Introducing a methyl group at position 3 to the *N*-linked benzyl group in compound **8b** diminished the antitumour activity (IC_{50} > 10 μM). The *N*-(4-fluorobenzyl)indoleamide **8c** exhibited approximately 2-fold higher cytotoxicity and antiproliferative activities (IC_{50} = 3.41 and 4.34 μM, respectively) compared to the unsubstituted amidobenzyl counterpart **8a**. Similar to **8b**, disubstituting the benzyl moiety at positions 2 and 3 with methoxy groups **8d** led to a drop in both cytotoxic and antiproliferative activities (IC_{50} > 10 μM). The *N*-piperonyl-indoleamide analogue **8e**, containing a 1,3-benzodioxole group in lieu of the phenyl ring in **8a**, was devoid of activity in the viability and proliferation assays (IC_{50} > 10 μM). Surprisingly, the *N*-homopiperonyl analogue **8f**, entailing an extra methylene group between the amide linkage and piperonyl motif, showed nearly 3.5-fold higher inhibitory activities (IC_{50} = 2.34 and 2.88 μM, respectively) compared to **8a** against KNS42 cells' viability and proliferation, respectively.

Bioisosteric replacement of the indole ring in reference compound **5** [IC_{50} (viability) = 0.33 μM] with a benzimidazole scaffold **10** resulted in a dramatic attenuation in the cytotoxic activity against KNS42 cells (IC_{50} > 10 μM). Of note, compound **10** previously showed high selective agonistic activity towards CB_2R (EC_{50} = 0.52 μM), without observable activity at CB_1R.[51] Nevertheless, unlike compounds **4** and **5**, compound **10** was inactive against KNS42 cells. Next, we evaluated the antitumour activity of benzimidazole derivatives **12a–c**, featuring a reversed amide linker. Akin to compound **10**, the benzimidazoleamide analogue **12a** failed to inhibit the viability and proliferation of KNS42 cells at 10 μM concentration. Introducing a methylene group spacer between the amide linker and the adamantane moiety in **12b** led to an improvement in the antiproliferative activity, while the cell viability remained unaffected (IC_{50} = 6.46 and > 10 μM, respectively). On the other hand, the benzimidazole-

Table 1 *In vitro* viability and proliferation inhibitory activities of compounds **8a–f**, **10**, **12a–c**, **14**, **18**, **23a** and **b**, **24a–e**, and **25a–e** as well as reference compounds **2–6** against KNS42 cells

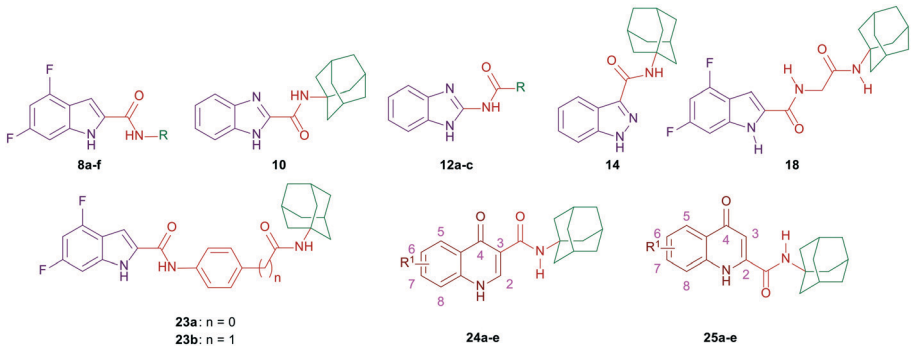

Cpd	R	R^1	Viability IC_{50} [a] (μM)	Proliferation IC_{50} [b] (μM)
8a	Benzyl	—	**8.25** ± 1.25	**9.85** ± 2.76
8b	3-Methylbenzyl	—	>10	>10
8c	4-Fluorobenzyl	—	**3.41** ± 0.49	**4.34** ± 0.46
8d	2,3-Dimethoxybenzyl	—	>10	>10
8e	Piperonyl	—	>10	>10
8f	Homopiperonyl	—	**2.34** ± 0.19	**2.88** ± 0.25
10	—	—	>10	>10
12a	Adamantane-1-yl	—	>10	>10
12b	1-Methyladamantane	—	>10	6.46
12c	4,6-Difluoroindole-2-yl	—	**4.49** ± 0.63	**4.03** ± 0.01
14			>10	>10
18	—	—	>10	>10
23a	—	—	>10	>10
23b	—	—	>10	4.90
24a	—	6-Chloro	>10	>10
24b	—	7-Bromo	>10	>10
24c	—	5,7-Dichloro	>10	9.17
24d	—	5,8-Dichloro	**9.06** ± 0.79	**2.92** ± 0.43
24e	—	7,8-Dichloro	>10	8.05 ± 4.15
25a	—	6-Chloro	>10	6.11 ± 0.91
25b	—	7-Bromo	>10	>10
25c	—	5,7-Dichloro	>10	>10
25d	—	5,8-Dichloro	>10	>10
25e	—	7,8-Dichloro	>10	>10
WIN55,212-2 (**2**)	—	—	8.02 ± 0.25	8.07 ± 0.29
JWH-133 (**3**)	—	—	>10	>10
4	—	—	4.75 ± 0.93	>10
5	—	—	0.33 ± 0.14	>10
6	—	—	5.04 ± 0.65	6.62 ± 2.01

[a] Compound dose required to achieve 50% inhibition of KNS42 cell viability, reflecting cytotoxicity. [b] Compound dose required to achieve 50% inhibition of KNS42 cell proliferation.

indole (BZ-IND) **12c** hybrid, linked through an amide group, equally inhibited the viability and proliferation of KNS42 cells (IC_{50} = 4.49 and 4.03 μM, respectively). In this hybrid, the indole-2-carboxamide framework integrated into compounds **8a–f** was preserved, while the benzimidazole nucleus served as the *N*-linked moiety which may explain the higher activity of this derivative compared to the other benzimidazole analogues **10**, **12a**, and **12b**.

Similar to the *N*-(adamantyl)benzimidazole derivative **10**, integrating an indazole scaffold, in place of the indole nucleus, into compound **14** led to a drastic drop in the cytotoxic activity against KNS42 cells (IC_{50} > 10 μM). It is worth noting that the same report which documented the CB_2R selective activity of compound **10** showed that compound **14** has higher agonistic activity towards CB_2R over CB_1R (CB_2R EC_{50} = 0.086 μM, CB_1R EC_{50} = 17.1 μM).[51] Thus far, the difference in the antitumour activity of **5** *versus* **10**, **12a**, and **14** suggests that the cytotoxic activity of the *N*-(adamantyl)indoleamide framework against KNS42 cells is superior to the benzimidazole and indazole counterparts. In addition, using the 4,6-difluoroindole scaffold in lieu of the unsubstituted indole ring featured in compound **5**, while concomitantly replacing the adamantane group therein with a 4-fluorobenzyl or homopiperonyl motif, was beneficial for the cytotoxic and antiproliferative activities against KNS42 cells.

Based on these findings and the potentiation of the antitumour activity seen in **8f** (upon extending the linker connecting the indole ring and the piperonyl motif), in our

subsequent round of evaluations, the 4,6-difluoroindole was maintained, while extra spacers were added in between the indole and adamantane moieties (Table 1). First, the adamantane-based indoledicarboxamide **18** showed no inhibitory activity against KNS42 cells in the viability and proliferation studies ($IC_{50} > 10$ μM). Similarly, in our previous report, compound **23a**, containing a phenyl group as a middle linker between the indole and adamantane rings, showed no activity at 10 μM concentration in both assays.[38] However, when we introduced an extra methylene spacer between the phenyl group and the amidoadamantyl motif in compound **23b**, a reduction in KNS42 cell proliferation was manifested (IC_{50} = 4.90 μM), while the cell viability remained unaffected. It is noteworthy that the antiproliferative activity of **23b** is comparable to that of our recently reported indoleamide **6** (IC_{50} = 6.62 μM), entailing a piperazine ring connecting the indole and the adamantane rings. These results suggest that stretching the middle linker connecting the indole and the adamantane moieties could be tolerated in certain structural settings.

The final modification in our study entailed replacing the indole ring in the *N*-(1-adamantyl)indoleamide framework with a quinolone moiety. Although the majority of the *N*-(1-adamantyl)quinolone-3-carboxamides that were reported to modulate the activity of CB receptors are *N*-alkylated at position 1 of the quinolone ring, few *N*-unsubstituted quinolone analogues were endowed with high affinity and selectivity for CB_2R.[41–44] Therefore, in accordance with our foregoing strategies, we assessed the cytotoxicity and antiproliferative activities of the adamantane-derived 1*H*-quinolone-3-carboxamides **24a–e**. Monosubstituted quinolones **24a** and **b** failed to inhibit the viability and proliferation of KNS42 cells at 10 μM concentration. Disubstituted quinolones **24c–e**, on the other hand, demonstrated good inhibitory activities against proliferation and/or viability of KNS42 cells. The 5,8-dichloroquinolone **24d** was the most active compound in this series with cytotoxicity (IC_{50} = 9.06 μM) and antiproliferative effects (IC_{50} = 2.92 μM) against KNS42 cells. The 5,7- and 7,8-disubstituted quinolones **24c** and **24e** exhibited IC_{50} values of 9.17 and 8.05 μM, respectively, in the proliferation assay, while they manifested lower inhibitory activities in the viability study ($IC_{50} > 10$ μM).

Shifting the amidoadamantyl motif from the 3-position of the quinolone scaffold to the 2-position in **25a–e** diminished the cytotoxic and antiproliferative activities ($IC_{50} > 10$ μM), except for compound **25a**. Unlike compound **24a**, the 6-chloroquinolone-2-carboxamide analogue **25a** showed only moderate antiproliferative activity against KNS42 cells (IC_{50} = 6.11 μM). Overall, the indole-2-carboxamide architecture appears to be preferable to the benzimidazole, indazole, and quinolone counterparts as antitumour agents.

4.1.2. Cytotoxicity and antiproliferative activities of the most potent compounds against different paediatric brain tumour cells and non-neoplastic fibroblasts. The top potent compounds in the viability and proliferation assays against KNS42 cells, **8a**, **8c**, **8f**, **12c**, and **24d** ($IC_{50} \leq 10$ μM) as well as WIN55,212-2 (**2**), were selected for further cytotoxicity and antiproliferative evaluations against a panel of grade IV paediatric brain tumour cells and non-neoplastic human fibroblasts (Table 2). All five compounds and WIN55,212-2 retained their viability and proliferation inhibitory activities ($IC_{50} \leq 10$ μM) against the two AT/RT tumour cell lines (BT12 and BT16). When tested against the medulloblastoma cells DAOY, the *N*-benzylindoleamide **8a** was devoid of antitumour activity ($IC_{50} > 10$ μM), as per our previous report.[38] However, the *N*-(4-fluorobenzyl)indole analogue **8c** demonstrated moderate cytotoxic activity (IC_{50} = 4.10 μM) and weak antiproliferative activity ($IC_{50} > 10$ μM) against DAOY cells. Similarly, the *N*-(homopiperonyl)-indoleamide analogue **8f** showed appreciable reduction of cell viability and moderate antiproliferative activity against DAOY cells (IC_{50} = 3.65 and 9.91 μM, respectively). Interestingly, the BZ-IND hybrid **12c** exhibited remarkable cytotoxic and antiproliferative activities against all tested paediatric tumour cells (KNS24, BT12, BT16, and DAOY). Compound **12c** also showed the most potent viability and proliferation inhibitory activities against DAOY cells (IC_{50} = 1.02 and 2.31 μM, respectively).

A similar pan-tumour cell viability and/or proliferation inhibition was manifested in the 5,8-dichloroquinolone-3-carboxamide derivative **24d** and WIN55,212-2. As we previously reported,[38] compound **8a**, which was cytotoxic against KNS42, BT12, and BT16 cells, exhibited limited cytotoxicity against healthy human fibroblasts, HFF1 cells (IC_{50} = 119 μM). Remarkably, compounds **8c**, **8f**, and **12c**, which demonstrated potent cytotoxicity against all paediatric brain tumour cell lines in our study, showed negligible cytotoxicity against HFF1 cells (IC_{50} = 281, 81, and 115 μM, respectively). However, compounds **8f** and **12c** inhibited the proliferation of HFF1 cells at concentrations < 10 μM. On the other hand, compound **24d** and WIN55,212-2 demonstrated potent viability and proliferation inhibitory activities against non-neoplastic HFF1 cells, indicating the non-selectivity and significant toxicity of these two compounds. Consistent with this observation, Ellert-Miklaszewska *et al.* also demonstrated that the increase of proapoptotic Bad protein activity is linked to WIN55,212-2's cytotoxic activity.[25]

4.2. Functional activity at the cannabinoid receptors

Given the structural resemblance of the synthesised molecules to the known cannabinoids, the most active compounds **8a**, **8c**, **8f**, **12c**, and **24d** in our study in addition to our recently reported indoleamide **6** were further evaluated *in vitro* for their ability to activate or antagonise human CB_1R and CB_2R expressed in mouse AtT-20 neuroblastoma cells (Table 3). All six compounds showed no agonistic activity at both CB receptors. These findings were in fact counterintuitive owing to the previously reported potent agonistic profile of the analogous two indoleamide reference compounds **4** and **5** as well as WIN55,212-2 (**2**). Nonetheless,

Table 2 *In vitro* cytotoxicity and antiproliferative effects of compounds **8a**, **8c**, **8f**, **12c**, and **24d** as well as WIN55,212-2 (**2**) against different paediatric brain cancer cell lines (BT12, BT16 and DAOY) and healthy human fibroblasts (HFF1)

Cpd	BT12 viability IC_{50}[a] (μM)	BT12 Prolif. IC_{50}[b] (μM)	BT16 viability IC_{50}[a] (μM)	BT16 Prolif. IC_{50}[b] (μM)	DAOY viability IC_{50}[a] (μM)	DAOY Prolif. IC_{50}[b] (μM)	HFF1 viability IC_5[a] (μM)	HFF1 Prolif. IC_{50}[b] (μM)
8a	**0.89** ± 0.12	**7.44** ± 0.59	**1.81** ± 0.21	**6.06** ± 0.69	>10	>10	119 ± 19.78	65 ± 8.73
8c	**9.23** ± 0.35	**8.87** ± 0.63	**5.50** ± 0.76	**9.79** ± 0.89	**4.10** ± 0.50	>10	281 ± 28.42	40 ± 9.81
8f	**6.08** ± 0.32	**4.10** ± 0.40	**2.72** ± 0.33	**7.53** ± 0.46	**3.65** ± 0.22	**9.91** ± 0.97	81 ± 20.26	6.98 ± 1.23
12c	**7.65** ± 0.38	**1.79** ± 0.21	**1.37** ± 0.13	**5.41** ± 0.55	**1.02** ± 0.07	**2.31** ± 0.38	115 ± 11.85	3.03 ± 0.55
24d	**5.15** ± 0.17	**3.59** ± 0.27	**1.96** ± 0.39	**4.88** ± 5.89	**1.54** ± 0.17	**4.71** ± 0.24	7.04 ± 0.87	3.85 ± 0.47
2	8.60 ± 0.78	9.32 ± 0.47	4.74 ± 3.77	4.57 ± 2.71	>10 ± 3.4	6.09 ± 0.22	0.023 ± 0.04	1.82 ± 0.42

[a] Compound dose required to achieve 50% inhibition of tumour/healthy cell viability, reflecting cytotoxicity. [b] Compound dose required to achieve 50% inhibition of tumour/healthy cell proliferation.

upon evaluating the antagonistic activity of **8a**, **8c**, **8f**, **12c**, and **24d** at CB_1R and CB_2R, we observed some mixed results. The indole-based dicarboxamide analogue **6** and the two *N*-(benzyl)indoleamide derivatives **8a** and **8c** failed to antagonise the response of CP55940, a non-selective CB_1R/CB_2R agonist. On the other hand, the *N*-(homopiperonyl) indoleamide **8f** potently inhibited the CP55940-mediated CB_1R activation with an IC_{50} value of 0.373 μM, whilst the CP55940-mediated CB_2R response remained unaffected at 10 μM concentration. The BZ-IND hybrid **12c** was inactive as an antagonist at both receptors. Contrary to compound **8f**, the quinolone-3-carboxamide **24d** failed to inhibit the CP55940-mediated response at CB_1R at 10 μM concentration while displaying potent antagonism at CB_2R (IC_{50} = 1.28 μM). These results suggest that the antitumour activities of our most potent compounds are unlikely to be a direct result of activity at CB_1R or CB_2R.

This was further corroborated by our previous highlights regarding the different cytotoxicity profiles of selective CB_2R agonists JWH-133 (**3**), **10** and **14** *versus* compounds **4** and **5** against KNS42 cells. In fact, the two *N*-benzylindoleamides **8a** and **8c** as well as the BZ-IND hybrid **12c** which exhibited potent antitumour profiles in our study showed no agonistic or antagonistic activity at both receptors. However, compounds **8f** and **24d** were shown in the functional assay to be CB ligands. Taken together, it is plausible that the antitumour activities observed in our compounds as well as WIN55,212-2 are not mediated by their action on CB receptors. Indeed, several studies have substantiated the CB-receptor independent induction of tumour cell death and antiproliferative effects exerted by many cannabinoids.

In this respect, in 1998, Sanchez *et al.* revealed that Δ^9-THC-induced apoptosis and sphingomyelin breakdown in C6 glioma cells (expressing CB_1R) were not prevented by the CB_1R antagonist SR141716. Their results suggested that the observed antitumour effects of Δ^9-THC are mediated through a CB_1R-independent mechanism.[22] This was further supported by Ruiz *et al.*'s findings in 1999 who also inferred that Δ^9-THC-induced apoptosis in human prostate tumour cells is independent of cannabinoid receptors.[50] However, Sanchez *et al.* showed in their subsequent reports that the three cannabinoids [Δ^9-THC (**1**), WIN55,212-2 (**2**), and JWH-133 (**3**)] induced apoptosis in C6 glioma cells *via* a CB_1R or CB_2R-dependent pathway, as well as sustained accumulation of pro-apoptotic ceramide.[24,29,30] Ensuing reports demonstrated that the antitumour activities of cannabinoids are independent of cannabinoid receptors.[26,31–36] These conflicting results highlight the elusive mechanism of action of cannabinoids as antitumour agents. Overall, the preceding findings suggest that the antitumour activity observed in our most potent analogues is likely independent of CB receptors.

Table 3 Functional profile of compounds **6**, **8a**, **8c**, **8f**, **12c**, and **24d** as well as cannabimimetic controls **2**, **4**, and **5**

	Agonism EC_{50} (μM)		Antagonism IC_{50} (μM)	
Cpd	CB_1R	CB_2R	CB_1R	CB_2R
6	NA[a]	NA[a]	NA[a]	NA[a]
8a	NA[a]	NA[a]	NA[a]	NA[a]
8c	NA[a]	NA[a]	NA[a]	NA[a]
8f	NA[a]	NA[a]	**0.373**	NA[a]
12c	NA[a]	NA[a]	NA[a]	NA[a]
24d	NA[a]	NA[a]	NA[a]	**1.28**
2	**0.284** (ref. 48)	**0.062** (ref. 48)	ND[b]	ND[b]
4	NA[a]	**0.12** (ref. 37)	NA[a]	NA[a]
5	NA[a]	**0.98** (ref. 37)	NA[a]	NA[a]

[a] NA: not active, defined as <50% activation or inhibition at 10 μM. [b] ND: not determined.

4.3. Differential gene expression analysis of KNS42 cells treated with compound 8a

In order to unravel the mechanism of action of the indole-2-carboxamides, we previously performed a transcriptional analysis on KNS42 cells treated with compound **6** *versus* the untreated control cell counterparts.[38] Upon examining the differential expression of the genes therein, we found that compound **6** downregulated the expression of two key genes, denominated carbonic anhydrase 9 (*CA9*) and spleen tyrosine kinase (*SYK*), with statistical significance ($p < 0.05$).[38] Indeed, since knocking down the activity of each of these two genes has been previously shown to inhibit the cell proliferation, invasion, and/or migration of GBM tumours, we concluded in our previous report that the antitumour activities of this

indoleamide molecule could be ascribed to repressing the expression of these two genes.[38] In the current study, we investigated the gene transcriptional response of KNS42 cells before and after they were treated with the *N*-benzylindoleamide **8a**, employing the DNBSEQ Eukaryotic Stranded Transcriptome Resequencing technique.

Inspecting the differential expression of the genes in the treated cells in comparison to the control cells revealed that compound **8a** downregulated the expression of 33 genes (fold change ≥5) with statistical significance ($p < 0.05$) (Table S1, ESI†). Seven genes were previously shown to promote the progression, proliferation, migration, and/or invasion of various tumours.[52–69] Accordingly, compound **8a**-induced downregulation of these genes could be the reason behind the antitumour attributes of this indoleamide against GBM KNS42 cells. Interestingly, neither the *CA9* nor *SYK* expression was significantly affected in **8a**-treated KNS42 cells.

These seven downregulated genes are: 1) placenta specific protein 1 (*PLAC1*), 2) Rho GTPase-activating protein 9 (*ARHGAP9*), 3) apelin early ligand A (*APELA*) gene, 4) NADH dehydrogenase [ubiquinone] 1 alpha subcomplex subunit 4-like 2 (*NDUFA4L2*), 5) mitogen-activated protein kinase 4 (*MAPK4*), 6) L-amino acid transporter 1 (*LAT1* or *SLC7A5*), and 7) angiopoietin-related protein 4 (*ANGPTL4*). It is noteworthy that the expression levels of *CNR1* and *CNR2* genes were not significantly altered in KNS42 cells treated with compound **6** or **8a**, further corroborating the premise that the CB receptors are presumably uninvolved in our observed antitumour activities. Importantly, upon retrospectively inspecting the differential gene expression data of KNS42 cells treated with our previously reported indoleamide analogue **6**, we did not observe any significant alteration in the expression levels of the preceding seven genes. Taken together, these findings suggest that despite both compounds **6** and **8a** bearing the same 4,6-difluoroindole-2-carboxamide structure core, the mechanisms through which they exert their antitumour effects are seemingly different.

First, *PLAC1*, the expression of which is restricted to placental tissues, wherein it plays a key role in the development and function of placenta, was previously found to be highly expressed and aberrantly activated in a wide variety of human cancers.[52–54,70] In addition, *PLAC1* serves as a biomarker signifying the presence and prognosis of certain tumours.[71–73] Indeed, apart from the placenta, no detectable expression of the *PLAC1* gene was found in any normal human tissues; therefore it is considered a cancer/placenta-specific gene and was designated as cancer-placenta antigen 1 (CP1).[54] A growing body of evidence has demonstrated the oncogenic potential of *PLAC1* in various human malignancies, where its expression was shown to be attributed to tumour progression.[52–54] Equally important, these studies revealed that silencing *PLAC1* in different cancer cells resulted in an inhibition in the proliferation and viability thereof, in addition to induction of apoptosis and cell cycle arrest. Knocking down *PLAC1* also impaired the migration and invasion of tumour cells which are metastasis-related phenomena that represent the hallmark of malignancy.[52–54] When the KNS42 cells were treated with **8a**, *PLAC1* was the most downregulated gene with high statistical significance (fold change = 30, $p < 0.005$). This profound suppression of *PLAC1* expression could have contributed to the observed cytotoxic and antiproliferative activities of compound **8a** against GBM KNS42 cells.

Two other genes that are potentially involved in the antitumour effects of **8a** are *ARHGAP9* and *MAPK4*. The protein encoded by *ARHGAP9* belongs to the Rho family of GTPases which principally modulate cytoskeletal dynamics.[55] Interestingly, ARHGAP9 was previously shown to serve as a docking protein for mitogen-activated protein kinases (MAPKs).[74] Indeed, the interaction observed between ARHGAP9 and MAPKs represents a key crosstalk mechanism between the Rho GTPase and MAPK signalling pathways that is potentially implicated in regulating actin remodelling.[74] It was, therefore, intriguing to find that *ARHGAP9* and *MAPK4* were downregulated in **8a**-treated KNS42 cells with high statistical significance (fold change = 12 and 6, respectively, $p < 0.0005$). However, whether the observed suppression of *ARHGAP9* and *MAPK4* expression is intertwined, or a mere coincidence requires further investigation. Of note, similar to *PLAC1*, the abnormal expression of *ARHGAP9* and *MAPK4* was found to be correlated with poor patient survival as well as the genesis and development/progression of various tumours.[55–58] Therefore, it has been proposed that both genes can be used as prognostic biomarkers for these tumours.[55,57] Within this context, Wang *et al.* demonstrated that silencing *ARHGAP9* in different human breast cancer cells resulted in a marked decrease in cell proliferation, migration, and invasion, as well as inducing cell cycle arrest and apoptosis thereof.[56] Similarly, knocking down the expression of *MAPK4* inhibited the proliferation and growth of different human tumour cells and xenografts.[57,58] Thus far, although the exact effects of *PLAC1*, *ARHGAP9*, and *MAPK4* expression in HGGs are yet to be determined, their highly significant downregulation in **8a**-treated KNS42 cells suggests, for the first time, their involvement in the tumorigenicity of the GBM tumours.

On the other hand, the oncogenic roles of *APELA*, *NDUFA4L2*, *SLC7A5*, and *ANGPTL4* in gliomas, including GBM, were previously demonstrated in the literature.[59,60,62,66,75] Accordingly, these four genes were highlighted by researchers as prospective therapeutic targets in malignant gliomas. The protein encoded by the *APELA* gene binds to the Apelin receptor and promotes the formation of human embryonic vasculature and the growth of embryonic stem cells.[59] Since many signalling networks function in both embryogenesis and cancers, Yi *et al.* investigated the expression of the *APELA* gene in normal tissues *vs.* cancer tissues.[61] They found that this gene is highly expressed in GBM tissues compared to LGGs. In the same study, the *APELA* overexpression in ovarian cancers was found to promote cell growth and migration as well as cell

cycle progression. Indeed, in the *APELA* knockout ovarian cancer cells, the loss of *APELA* led to an inhibition in cell proliferation and migration *in vitro*. Similar results were discerned in a model of ovarian cancer xenograft bearing mice, in which the size of *APELA* knockout tumours was significantly decreased compared to the wild-type tumours, supporting the role of *APELA* in ovarian cancer growth and progression and suggesting its pro-tumorigenic effects *in vivo*.[61]

In a subsequent report by Ganguly *et al.*, *APELA* was found to be expressed at high levels in glioma patients and its upregulation was negatively correlated with patient survival.[59] In this respect, there was a significant difference between high and low *APELA* expressing glioma patients, with high *APELA* expression being associated with poor patient survival. In fact, the authors showed a direct correlation between *APELA* expression and glioma grade, wherein the highest *APELA* expression was found in GBM tumours (grade IV), in resonance with Yi *et al.*'s findings.[59,61] Interestingly, unlike the *APELA* gene, the expression of the Apelin receptor gene in these patients was not associated with glioma grade or survival rates.[59] The significant downregulation of *APELA* in **8a**-treated KNS42 cells (fold change = 11, $p < 0.05$) accorded with the preceding findings, supporting the role of *APELA* in the growth of GBM tumours and suggesting that its suppression in KNS42 cells likely contributed to the observed antitumour effects of **8a**.

Similar to *APELA*, *NDUFA4L2* was shown to act as an oncogene in different tumours, including GBM.[60] NDUFA4L2 is a subunit of the mitochondrial respiratory chain complex I, which is implicated in oxidative stress and metabolic reprograming in various cancers. Indeed, many interesting findings were documented in a very recent study, published in 2021, supporting the role of *NDUFA4L2* in promoting GBM progression.[60] Chen *et al.* reported therein that the NDUFA4L2 mRNA and protein were markedly upregulated in human GBM tissues and these elevated levels were associated with shorter survival times in GBM patients. Therefore, they suggested that the high expression of *NDUFA4L2* can be regarded as an independent prognostic biological marker for the overall survival of GBM patients.[60] Like *APELA*, the expression levels of *NDUFA4L2* in GBM tissues were found to be highly increased, compared to LGGs and normal brain tissues. More importantly, they found that knocking down the *NDUFA4L2* gene, both *in vitro* and *in vivo*, suppressed tumour cell proliferation and increased apoptosis, whilst protective mitophagy was initiated. They also discovered that apatinib, a multikinase inhibitor that displayed promising antitumour effects in various clinical trials, can effectively target *NDUFA4L2*, recapitulating the effects brought forth by *NDUFA4L2* gene knockdown.[60] Indeed, apatinib efficiently reduced the expression of *NDUFA4L2*, causing cell cycle arrest, enhanced apoptosis, and initiation of protective mitophagy, both *in vitro* and *in vivo*. This study was the first to demonstrate the tumorigenic role of *NDUFA4L2* in GBM tumours.[60] Interestingly, compound **8a** inhibited the expression of *NDUFA4L2* by 7-fold with high statistical significance ($p < 0.0005$). Resonating with the preceding antitumour characteristics of apatinib, **8a**-induced downregulation of *NDUFA4L2* likely contributed to the observed antiproliferative and cytotoxic effects of **8a** against GBM cells.

The next gene that we determined to be potentially implicated in **8a**-induced antitumour effects is *SLC7A5*, also referred to as *LAT1*. This gene belongs to system L transporters, which is accountable for the cellular uptake of most essential amino acids.[76] *LAT1* was found to be upregulated in various types of cancer, with predominant expression in metastatic lesions and primary tumours; therefore it is considered a cancer-type amino acid transporter.[76] Indeed, its high expression was previously shown to be closely related to growth, progression, and aggressiveness of different tumours.[62–65] Therefore, it was also suggested that *LAT1* can be used as an independent marker for poor prognosis in different types of cancer.[63] Its tumour-promoting activity was proven *in vivo* when *LAT1* knockdown metastatic prostatic cancer xenografts showed suppressed cell cycle progression, tumour growth, and spontaneous metastasis.[64] Importantly, accumulating literature reports have highlighted several LAT1 inhibitors that displayed reduction of cellular uptake of leucine, tumour cell proliferation, and cell cycle progression in various cancer cell lines *in vitro*, as well as inhibiting tumour growth *in vivo*.[63,76,77] Within this context, Kobayashi *et al.* demonstrated that 2-aminobicyclo-(2, 2, 1)-heptane-2-carboxylic acid (BCH), a classical LAT1 inhibitor, displayed remarkable cytostatic (reduced proliferation) and cytocidal (increased apoptosis) effects in glioma cells overexpressing the *LAT1* gene.[62] They also found that increasing the expression of *LAT1* significantly enhanced the rate of tumour growth in glioma cells with low endogenous expression of *LAT1* in mice. Additionally, *LAT1* was found to be expressed at higher levels in human HGGs, including GBM, compared to LGGs, while being undetected in non-neoplastic brain tissues, correlating the expression levels of *LAT1* with the malignant status of glioma.[62] This was further substantiated by Haining *et al.*'s study which associated *LAT1* upregulation with the histopathological grade, proliferation, and angiogenesis of gliomas, in addition to the poor prognosis of glioma patients.[66] The 5-fold downregulation of *LAT1* with a very high statistical significance ($p < 0.0001$) manifested in **8a**-treated KNS42 cells, together with the aforementioned compelling findings, supports the possible involvement of *LAT1* in the proliferation and viability inhibition of GBM cells induced by **8a**.

Finally, we found that *ANGPTL4* was 5-fold downregulated in **8a**-treated KNS42 cells with statistical significance ($p < 0.05$). This gene is involved in numerous physiological and pathological functions, such as lipid metabolism, angiogenesis, cell differentiation, and tumorigenesis.[78] Several studies demonstrated that high levels of *ANGPTL4* are correlated with poorer prognosis in patients with solid

tumours, including GBM, suggesting its role in cancer onset, angiogenesis, progression, and metastasis.[67–69] Importantly, Katanasaka *et al.* showed that upregulating the expression of *ANGPTL4* promotes tumour angiogenesis in GBM.[75] In addition, constitutive knockdown of the *ANGPTL4* gene in GBM cells resulted in a significant reduction in the angiogenesis and growth of the corresponding tumour xenografts. This in turn suggests the likely involvement of this gene in the antitumour effects detected in compound **8a**.

Overall, we identified seven genes whose expression levels were previously correlated with growth, progression, and poor prognosis of various tumours. Targeting the activity of each of these seven genes genetically and/or chemically was also shown to abrogate tumour growth in several reports. Accordingly, the antitumour activity of **8a** could be accredited to modulating the expression levels of these oncogenes.

4.4. ADME profiling

The top potent derivatives **8a**, **8c**, **8f**, **12c**, and **24d** in addition to WIN55,212-2 (**2**) were evaluated for their drug-likeness (Table 4) through assessing their conformity to Lipinski's rule of five (RO5) using ACD/Labs Percepta 2016 Build 2911 (13 Jul 2016). The log BB values of these compounds were also predicted *in silico* to examine their BBB permeability potential. The indole-2-carboxamide derivatives **8a**, **8c**, **8f**, and **12c** as well as WIN55,212-2 showed no violation to the RO5, indicating the drug-like attributes of these compounds. The small size and optimum lipophilicity (Log P = 2.69–3.23) of the preceding four indole-2-carboxamides suggest the prospective bioavailability of these analogues. On the contrary, the high lipophilicity of the quinolone derivative **24d** (log P = 5.07) accounted for the one minor violation observed therein. All five compounds and WIN55,212-2 (**2**) are also expected to traverse the BBB, whereupon they may exert their antitumor activities.

5. Conclusions

Motivated by the previously reported antitumour activity of the indole-based CB ligands WIN55,212-2 and compound **5**, several analogous arylcarboxamide derivatives were designed, synthesised and evaluated for their cytotoxicity and antiproliferative activities against paediatric GBM KNS42 cells. The structure–antitumour activity relationship of our analogues led to the following highlights: (a) the indole-2-carboxamide framework is superior to the benzimidazole, indazole and quinolone counterparts; (b) replacing the adamantane moiety in **5** with benzyl or homopiperonyl groups was favourable; (c) mixed results were manifested when the linker connecting the indole moiety and adamantane group was overextended. Derivatives **8a**, **8c**, **8f**, **12c**, and **24d** displayed the most potent inhibitory activities against the viability and proliferation of KNS42 cells. WIN55,212-2 and selective CB_2R agonists **4** and **5** showed potent cytotoxic activities against KNS42 cells, whilst JWH-133 was devoid of activity. Compounds **8a**, **8c**, **8f**, **12c**, and **24d** maintained their potent antitumour activities against the other tested grade IV non-GBM paediatric brain tumour cells BT12 and BT16 (AT/RT). When tested against the DAOY (medulloblastoma) cells, these compounds were mostly active, with the exception of **8a**. All indole-2-carboxamides **8a**, **8c**, **8f**, and **12c** showed no cytotoxicity against non-neoplastic human fibroblasts HFF1, suggesting their selective activity towards tumour cells. On the contrary, the quinolone-3-carboxamide **24d** and reference compound WIN55,212-2 were toxic towards HFF-1 cells.

Based on the structural similarities between the newly synthesised compounds and known indole-based cannabinoids, CB functional assays were performed. None of our five most active compounds showed agonistic activity at CB_1R or CB_2R. In the antagonist mode, compounds **8a**, **8c**, and **12c** failed to inhibit the CP55940-mediated response at both receptors. On the contrary, compounds **8f** and **24d** behaved as antagonists at CB_1R and CB_2R, respectively. The discrepancies observed between the antitumour activities of our compounds and their CB functional profiles suggest a complex interplay between CB receptor modulation and CB-independent antitumour mechanisms which remain to be determined. This was further supported by previous reports indicating the non-involvement of CB receptors in the antitumour activity of several cannabinoids.[22,26,31–36,50,79] We further substantiated this premise when we performed a transcriptional analysis on KNS42 cells, wherein neither compound **6** nor **8a** altered the expression of *CNR1* and *CNR2* genes. Contrary to our recent findings on compound **6**,[38] the *N*-benzylindoleamide **8a** did not show a significant modification in the expression of *CA9* and *SYK* genes. Alternatively, we found a set of seven oncogenes that were significantly downregulated in **8a**-treated KNS42 cells.

The expression levels of each of these seven genes was previously shown to be positively correlated with the growth, progression, migration, invasion, and/or prognosis of various tumours.[52–64,66–69] Since genetically and/or chemically inhibiting the expression of these genes has been previously shown to suppress tumour growth, the antitumour activity of **8a** could be attributed to downregulating the expression of

Table 4 Calculated drug-like properties of the top potent compounds **8a**, **8c**, **8f**, **12c**, and **24d** in addition to reference compound **2** using ACD/Labs Percepta 2016 build 2911 (13 Jul 2016)

Cpd	MW	HBD	HBA	log P	NRB	TPSA	Log BB
8a	286.28	2	3	3.17	3	44.89	0.08
8c	304.27	2	3	3.23	3	44.89	−0.20
8f	344.31	2	5	3.02	4	63.35	−0.15
12c	312.27	3	5	2.69	2	73.57	−0.64
24d	391.29	2	4	5.07	2	58.20	0.21
2	426.51	0	5	4.13	4	43.70	−0.23

MW: molecular weight, HBD: H-bond donors, HBA: H-bond acceptors, log P: octanol–water partition coefficient, NRB: number of rotatable bonds, TPSA: topological polar surface area, Log BB: [log (C brain/C blood)].

these genes. Upon performing a retrospective examination on the differential expression of the genes in compound **6**-treated KNS42 cells, we found that the expression levels of the seven genes, potentially implicated in **8a** antitumour activity, are not significantly changed. This in turn suggests that despite the structural homology between compounds **6** and **8a**, both compounds seemingly inhibit the proliferation and viability of GBM cells *via* different mechanisms of action. Overall, the drug-like profile, *in vitro* antitumour activities, and preliminary safety towards non-tumour cells of **8a**, **8c**, **8f**, and **12c** establish the indole-2-carboxamides as potential therapeutic agents that can efficiently target malignant brain tumours.

6. Experimental section

6.1. Chemistry

General information. The following starting materials: 4,6-difluoroindole-2-carboxylic acid (**7**) and 1-adamantylamine (**15**) were purchased from Fluorochem, while 2-aminobenzimidazole (**11**) was purchased from AlfaAesar. Benzimidazole-2-carboxylic acid (**9**), indazole-3-carboxylic acid (**13**), and 4-aminophenylacetic acid (**19b**) were purchased from AK Scientific. WIN55,212-2 and JWH-133 were purchased from Cayman Chemical. ^{1}H NMR and ^{13}C NMR spectra were recorded on a Bruker Avance III spectrometer at 400 and 100 MHz, respectively, with TMS as an internal standard. Standard abbreviations indicating multiplicity were as follows: s = singlet, d = doublet, dd = doublet of doublets, t = triplet, q = quadruplet, m = multiplet and br = broad. HRMS experiments were carried out on a Thermo Scientific Q-Exactive Orbitrap mass spectrometer. TLC was performed on Analtech silica gel TLC plates (200 microns, 20 × 20 cm). Flash chromatography was conducted using a Teledyne Isco CombiFlash Rf system with RediSep columns or manually using SiliCycle SiliaFlash® P60 silica gels [40–63 μm (230–400 mesh)]. The final compounds were purified by preparative HPLC unless otherwise stated. The preparative HPLC employed an Omega 5 μm Polar C18 (21.2 × 150 mm) column, with detection at 254 and 280 nm on a Shimadzu SPD-20A detector, flow rate = 25.0 mL min^{-1}. Method 1: 40–100% acetonitrile/H_2O in 10 min; 100% acetonitrile in 15 min; 100–40% acetonitrile/H_2O in 10 min. Method 2: 50–100% acetonitrile/H_2O in 10 min; 100% acetonitrile in 15 min; 100–50% acetonitrile/H_2O in 10 min. Method 3: 60–100% acetonitrile/H_2O in 10 min; 100% acetonitrile in 15 min; 100–60% acetonitrile/H_2O in 10 min. Both solvents contained 0.05 vol% of trifluoroacetic acid (TFA). The purities of the final compounds were established by analytical HPLC, which was carried out using a Waters 1525 HPLC system with a Phenomenex 5 μm C18 (2) (150 × 4.6 mm), on a Waters 2487 dual wavelength detector. Analytical HPLC method: flow rate = 1 mL min^{-1}; gradient elution over 35 min. Gradient: 20–100% acetonitrile/H_2O in 15 min; 100% acetonitrile in 10 min; 100–20% acetonitrile/H_2O in 5 min. Both solvents incorporated 0.05 vol% of TFA. The purity of all tested compounds was at least 95% as determined by the method described above.

6.1.1. General procedure for amide coupling (method A). To a solution of the appropriate carboxylic acid (1 equiv.) in anhydrous dimethylformamide (DMF, 10 mL mmol^{-1}), HOBt (2 equiv.) and EDC·HCl (2 equiv.) were added at room temperature (rt). After stirring for 10 min, the corresponding amine (1.2 equiv.) and DIPEA (6 equiv.) were added, and the reaction mixture was stirred at room temperature (rt) until the disappearance of the starting material (usually 60–72 h). After this time, water (50 mL) was added, and the mixture was extracted with EtOAc (3 × 50 mL). The combined organic layers were washed with water (5 × 25 mL) and brine (1 × 25 mL), dried over anhydrous Na_2SO_4, filtered, and concentrated under reduced pressure. The residue was purified by flash chromatography using a dichloromethane/methanol (DCM/MeOH) gradient prior to further preparative HPLC purification unless otherwise stated.

6.1.2. General procedure for amide coupling (method B). A mixture of 2-aminobenzimidazole (1 mmol), EDC·HCl (1.2 mmol), DMAP (1.2 mmol) and the appropriate carboxylic acid (1.2 mmol) in a (1 : 1) 20 mL mixture of anhydrous DCM and anhydrous tetrahydrofuran (THF) was stirred at room temperature (rt) for 72 h. In compounds **12a** and **12c**, the reaction mixture was quenched with saturated NH_4Cl solution (50 mL) and extracted with DCM (3 × 25 mL) and ethyl acetate (3 × 25 mL). The combined organic layers were washed with brine (1 × 50 mL), dried over anhydrous Na_2SO_4, filtered, and concentrated under reduced pressure. The residue was purified by flash chromatography using a DCM/MeOH gradient. The two compounds were then further purified *via* preparative HPLC to attain >95% purity. In compound **12b**, after 72 h of stirring at rt, the solvent was evaporated under vacuum and the residue was purified by manual column chromatography. The obtained product was already >95% pure.

6.1.3. General procedure for *N*-Boc protection (method C). To a solution of the appropriate amine (3 mmol) in 30 mL of water : dioxane (1 : 2), di-*tert*-butyl dicarbonate (Boc_2O, 6 mmol) and triethylamine (Et_3N, 6 mmol) were added and the reaction mixture was stirred at rt for 72 h. Three quarters of the solvent was then evaporated *in vacuo* and the residue was acidified with 3 M aqueous HCl. The formed precipitate was filtered off, washed with water, and dried.

6.1.4. General procedure for *N*-Boc deprotection (method D). To a solution of the *N*-Boc protected amine (1 mmol) in 5 mL DCM, 2 mL TFA was added. The reaction mixture was stirred for 12 h and concentrated *in vacuo* then Na_2HCO_3 solution was added for neutralisation, followed by extraction with DCM (3 × 50 mL). The combined organic phases were washed with brine (1 × 25 mL), dried over anhydrous Na_2SO_4, filtered, and concentrated under reduced pressure. The residue was purified by flash chromatography using a DCM/MeOH gradient.

6.1.5. Preparation of synthetic intermediates 20a, 21a, 22a, and final compound 23a. The synthesis of the title

compounds and their chemical characterisation are delineated in our recent article.[38]

6.1.6. Preparation of the tested quinoloneamides. The tested quinolones **24a–e** and **25a–e** were synthesised and characterised as we previously reported.[46]

*N-Benzyl-4,6-difluoro-1H-indole-2-carboxamide (**8a**).* This compound was obtained from 4,6-difluoroindole-2-carboxylic acid (**7**) and benzylamine employing method A. White solid, yield: 98%. Its chemical characterisation is detailed in our recently published report.[38] ^{1}H NMR (DMSO-d_6) δ 12.05 (s, 1H), 9.13 (t, J = 5.9 Hz, 1H), 7.38–7.28 (m, 5H), 7.28–7.20 (m, 1H), 7.04 (dd, J = 9.4, 1.3 Hz, 1H), 6.87 (td, J = 10.4, 1.9 Hz, 1H), 4.52 (d, J = 6.0 Hz, 2H).

*4,6-Difluoro-N-(3-methylbenzyl)-1H-indole-2-carboxamide (**8b**).* 4,6-Difluoroindole-2-carboxylic acid (**7**) and 3-methylbenzyl amine were used to deliver the title compound following method A. It was >95% pure after flash chromatography. White solid, yield: 90%.^{1}H NMR (DMSO-d_6) δ 12.04 (s, 1H), 9.09 (t, J = 6.0 Hz, 1H), 7.30 (s, 1H), 7.22 (t, J = 7.5 Hz, 1H), 7.17–7.00 (m, 4H), 6.87 (td, J = 10.4, 1.8 Hz, 1H), 4.49 (d, J = 6.0 Hz, 2H); ^{13}C NMR (DMSO-d_6) δ 160.8, 159.7 (dd, J = 237.0, 12.0 Hz), 156.2 (dd, J = 248.7, 15.5 Hz), 139.7138.1 (dd, J = 15.2, 13.2 Hz), 137.9, 133.1 (d, J = 3.2 Hz), 128.7, 128.3, 128.0, 124.8, 113.6 (d, J = 21.9 Hz), 98.8, 95.7 (dd, J = 29.7, 23.2 Hz), 95.1 (dd, J = 25.9, 4.4 Hz), 42.7, 21.5; HRMS (ESI) m/z calcd for $C_{17}H_{14}F_2N_2O$ ($[M + H]^+$) m/z 301.1147; found 301.1141.

*4,6-Difluoro-N-(4-fluorobenzyl)-1H-indole-2-carboxamide (**8c**).* The title compound was obtained from 4,6-difluoroindole-2-carboxylic acid (**7**) and 4-fluorobenzyl amine employing method A. This compound was purified by crystallisation from DMF and was obtained in >95% purity. Off white solid, yield: 76%.^{1}H NMR (DMSO-d_6) δ 12.04 (s, 1H), 9.13 (t, J = 6.0 Hz, 1H), 7.46–7.33 (m, 2H), 7.27 (s, 1H), 7.21–7.11 (m, 2H), 7.03 (dd, J = 9.4, 1.5 Hz, 1H), 6.88 (td, J = 10.4, 2.0 Hz, 1H), 4.49 (d, J = 5.9 Hz, 2H); ^{13}C NMR (DMSO-d_6) δ 161.7 (d, J = 242.3 Hz), 160.8, 159.7 (dd, J = 237.0, 12.0 Hz), 156.2 (dd, J = 248.8, 15.6 Hz), 138.1 (dd, J = 15.0, 13.3 Hz), 136.0 (d, J = 3.0 Hz), 133.0 (d, J = 3.1 Hz), 129.7 (d, J = 8.1 Hz), 115.5 (d, J = 21.3 Hz), 113.6 (d, J = 21.8 Hz), 98.9, 95.7 (dd, J = 29.7, 23.3 Hz), 95.1 (dd, J = 25.9, 4.3 Hz), 42.0; HRMS (ESI) m/z calcd for $C_{16}H_{11}F_3N_2O$ ($[M + H]^+$) m/z 305.0896; found 305.0894.

*N-(2,3-Dimethoxybenzyl)-4,6-difluoro-1H-indole-2-carboxamide (**8d**).* This compound was synthesised from 4,6-difluoroindole-2-carboxylic acid (**7**) and 2,3-dimethoxybenzyl amine following method A. White solid, yield: 78%.^{1}H NMR (DMSO-d_6) δ 12.05 (s, 1H), 9.07 (t, J = 5.9 Hz, 1H), 7.29 (s, 1H), 7.03 (dd, J = 9.4, 1.3 Hz, 1H), 6.97 (d, J = 1.5 Hz, 1H), 6.85–6.92 (m, 3H), 4.44 (d, J = 5.9 Hz, 2H), 3.74 (s, 3H), 3.72 (s, 3H); ^{13}C NMR (DMSO-d_6) δ 160.7, 159.6 (dd, J = 238.3, 12.1 Hz), 156.2 (dd, J = 248.6, 15.6 Hz), 149.1, 148.3, 138.1 (dd, J = 15.2, 13.3 Hz), 133.2 (d, J = 3.2 Hz), 132.2, 120.0, 113.6 (d, J = 22.0 Hz), 112.3, 112.0, 98.9, 95.6 (dd, J = 29.7, 23.2 Hz), 95.1 (dd, J = 25.9, 4.4 Hz), 56.0, 55.9, 42.5; HRMS (ESI) m/z calcd for $C_{18}H_{16}F_2N_2O_3$ ($[M + H]^+$) m/z 347.1202; found 347.1202.

*N-(Piperonyl)-4,6-difluoro-1H-indole-2-carboxamide (**8e**).* This compound was obtained from 4,6-difluoroindole-2-carboxylic acid (**7**) and piperonylamine following method A. It was 95% pure after flash chromatography. Buff solid, yield: 93%.^{1}H NMR (DMSO-d_6) δ 12.03 (s, 1H), 9.05 (t, J = 6.0 Hz, 1H), 7.26 (s, 1H), 7.02 (dd, J = 9.4, 1.5 Hz, 1H), 6.93–6.84 (m, 3H), 6.81 (dd, J = 8.0, 1.5 Hz, 1H), 5.98 (s, 2H), 4.41 (d, J = 6.0 Hz, 2H); ^{13}C NMR (DMSO-d_6) δ 160.7, 159.7 (dd, J = 238.4, 12.2 Hz), 156.2 (dd, J = 248.7, 15.5 Hz), 147.7, 146.6, 138.1 (dd, J = 15.3, 13.2 Hz), 133.7, 133.1 (d, J = 3.3 Hz), 121.0, 113.6 (d, J = 22.5 Hz), 108.5, 108.4, 101.3, 98.8, 95.7 (dd, J = 29.7, 23.3 Hz), 95.1 (dd, J = 25.8, 4.4 Hz), 42.5; HRMS (ESI) m/z calcd for $C_{17}H_{12}F_2N_2O_3$ ($[M + H]^+$) m/z 331.0889; found 331.0881.

*N-(Homopiperonyl)-4,6-difluoro-1H-indole-2-carboxamide (**8f**).* The title compound was synthesised from 4,6-difluoroindole-2-carboxylic acid (**7**) and homopiperonylamine following method A. It was >95% pure after flash chromatography. White solid, yield: 73%.^{1}H NMR (DMSO-d_6) δ 11.97 (s, 1H), 8.60 (t, J = 5.6 Hz, 1H), 7.19 (d, J = 1.1 Hz, 1H), 7.02 (dd, J = 9.4, 1.4 Hz, 1H), 6.88 (overlapping td, J = 10.4, 2.0 Hz, 1H), 6.84 (d, J = 1.6 Hz, 1H), 6.81 (d, J = 7.9 Hz, 1H), 6.69 (dd, J = 7.9, 1.6 Hz, 1H), 5.95 (s, 2H), 3.47 (q, J = 6.7 Hz, 2H), 2.77 (t, J = 7.2 Hz, 2H); ^{13}C NMR (DMSO-d_6) δ 160.7, 159.6 (dd, J = 238.3, 12.1 Hz), 156.1 (dd, J = 248.5, 15.6 Hz), 147.7, 146.0, 138.0 (dd, J = 15.2, 13.2 Hz), 133.6, 133.3 (d, J = 3.3 Hz), 122.0, 113.6 (d, J = 21.1 Hz), 109.5, 108.6, 101.1, 98.5, 95.6 (dd, J = 29.6, 23.3 Hz), 95.1 (dd, J = 25.9, 4.4 Hz), 41.1, 35.2; HRMS (ESI) m/z calcd for $C_{19}H_{20}F_2N_2O_2$ ($[M + H]^+$) m/z 345.1045; found 345.1038.

*N-(1-Adamantyl)-1H-benzimidazol-2-carboxamide (**10**).* The title compound was synthesised from benzimidazole-2-carboxylic acid (**9**) and 1-adamantylamine following method A. The ^{1}H NMR data matched the one reported in the literature.[51] It was >95% pure after flash chromatography. White solid, yield: 66%. ^{1}H NMR (DMSO-d_6) δ 13.11 (s, 1H), 7.74 (s, 1H), 7.61 (s, 2H), 7.31–7.24 (m, 2H), 2.10 (s, 6H), 2.08 (s, 3H), 1.67 (s, 6H).

*N-(1H-Benzimidazol-2-yl)adamantane-1-carboxamide (**12a**).* The title compound was synthesised from 2-aminobenzimidazole (**11**) and 1-adamantanecarboxylic acid according to method B and its ^{1}H NMR data matched the one we reported before.[80] White solid, yield: 41%. The ^{1}H NMR (DMSO-d_6) δ 7.61 (s, 2H), 7.32 (s, 2H), 2.05 (s, 3H), 1.97 (s, 6H), 1.72 (s, 6H).

*2-(1-Adamantyl)-N-(1H-benzimidazol-2-yl)acetamide (**12b**).* This compound was obtained from 2-aminobenzimidazole (**11**) and 1-adamantaneacetic acid employing method B and it was >95% pure after flash chromatography. Its ^{1}H NMR data matched the one we reported before.[80] White solid, yield: 72%.^{1}H NMR (DMSO-d_6) δ 12.05 (s, 1H), 11.41 (s, 1H), 7.43 (s, 2H), 7.15–6.95 (m, 2H), 2.19 (s, 2H), 1.91 (s, 3H), 1.74–1.49 (m, 12H).

*N-(1H-Benzimidazol-2-yl)-4,6-difluoro-1H-indole-2-carboxamide (**12c**).* This compound was obtained *via* amide coupling 2-aminobenzimidazole (**11**) and 4,6-difluoroindole-2-carboxylic acid (**6**) following method B. White solid, yield:

35%. ^{1}H NMR (DMSO-d_6) δ 12.34 (s, 1H), 7.67 (s, 1H), 7.62 (s, 2H), 7.32 (dd, J = 5.3, 2.2 Hz, 2H), 7.14 (dd, J = 9.3, 1.8 Hz, 1H), 6.96 (td, J = 10.3, 2.0 Hz, 1H); ^{13}C NMR (DMSO-d_6) δ 160.8, 160.6 (dd, J = 240.5, 12.0 Hz), 156.6 (dd, J = 250.3, 15.6 Hz), 146.3, 139.1 (overlapping dd, J = 14.0 Hz, 1H), 131.4, 124.0, 113.9, 113.8, 113.7, 102.8, 96.4 (dd, J = 30.0, 23.0 Hz), 95.4 (dd, J = 26.0, 4.1 Hz); HRMS (ESI) m/z calcd for $C_{17}H_{14}F_2N_2O$ ([M + H]$^+$) m/z 301.1147; found 301.1141.

*N-(1-Adamantyl)-1H-indazole-3-carboxamide (**14**).* The title compound was synthesised from indazole-3-carboxylic acid (**13**) and 1-adamantylamine following method A. It was >95% pure after flash chromatography. The ^{1}H NMR data matched the one reported in the literature.[51] White solid, yield: 62%. ^{1}H NMR (DMSO-d_6) δ 13.47 (s, 1H), 8.14 (d, J = 8.2 Hz, 1H), 7.59 (d, J = 8.4 Hz, 1H), 7.40 (t, J = 7.6 Hz, 1H), 7.27–7.17 (m, 2H), 2.11 (s, 6H), 2.07 (s, 3H), 1.68 (s, 6H).

*tert-Butyl (2-(adamantan-1-ylamino)-2-oxoethyl)carbamate (**16**).* The title compound was prepared from 1-adamantylamine (**15**) according to the reported procedure.[47] The obtained crude residue was used without further purification in the next step; white solid, yield: 80%.

*N-(1-Adamantyl)-2-aminoacetamide (**17**).* This compound was synthesised using the crude product **16** employing method D. The ^{1}HNMR data matched the one reported in the literature.[47] White solid, yield: 92%. ^{1}H NMR (DMSO-d_6) δ 7.48 (s, 1H), 3.12 (s, 2H), 2.01 (s, 3H), 1.92 (d, J = 2.6 Hz, 6H), 1.62 (s, 6H).

*N-(2-((Adamantan-1-yl)amino)-2-oxoethyl)-4,6-difluoro-1H-indole-2-carboxamide (**18**).* This compound was prepared from compound **17** and 4,6-difluoroindole-2-carboxylic acid (**7**) following method A. White solid, yield: 82%.^{1}H NMR (DMSO-d_6) δ 12.02 (s, 1H), 8.71 (t, J = 5.9 Hz, 1H), 7.38 (s, 1H), 7.25 (d, J = 1.7 Hz, 1H), 7.04 (dd, J = 9.3, 1.5 Hz, 1H), 6.88 (td, J = 10.4, 1.8 Hz, 1H), 3.85 (d, J = 5.9 Hz, 2H), 2.01 (s, 3H), 1.94 (s, 6H), 1.62 (s, 6H); ^{13}C NMR (DMSO-d_6) δ 168.0, 161.0, 159.7 (dd, J = 238.5, 12.1 Hz), 156.2 (dd, J = 248.7, 15.5 Hz), 138.1 (dd, J = 15.2, 13.2 Hz), 133.0 (d, J = 3.3 Hz), 113.6 (d, J = 21.7 Hz), 99.0, 95.7 (dd, J = 29.6, 23.3 Hz), 95.0 (dd, J = 25.9, 4.4 Hz), 51.3, 42.8, 41.5, 36.5, 29.3; HRMS (ESI) m/z calcd for $C_{21}H_{23}F_2N_3O_2$ ([M + H]$^+$) m/z 388.1831; found 388.1830.

*2-(4-((tert-Butoxycarbonyl)amino)phenyl)acetic acid (**20b**).* This compound was obtained *via* *N*-Boc protection of 4-aminophenylacetic acid **19b** following method C. The ^{1}HNMR data matched the one reported in the literature.[81] White solid, yield: 84%.^{1}H NMR (DMSO-d_6) δ 7.89 (d, J = 8.2 Hz, 2H), 7.45 (t, J = 6.0 Hz, 1H), 7.34 (d, J = 8.2 Hz, 2H), 4.18 (d, J = 6.1 Hz, 2H), 1.39 (s, 9H).

*tert-Butyl (4-(2-((-adamantan-1-yl)amino)-2-oxoethyl)phenyl) carbamate (**21b**).* The title compound was prepared *via* amide coupling **20b** and 1-adamantylamine employing method A. The collected crude product after evaporating the EtOAc extract was used without further purification in the next step; buff solid, yield: 70%.

*N-(1-Adamantyl)-2-(4-aminophenyl)acetamide (**22b**).* This compound was obtained *via* *N*-Boc deprotection (method D) of the crude product **21b**. Buff solid, yield: 90%.^{1}H NMR (DMSO-d_6) δ 10.06 (t, J = 5.7 Hz, 1H), 7.74 (d, J = 8.2 Hz, 2H), 7.54 (s, 1H), 7.31 (d, J = 8.2 Hz, 2H), 4.42 (d, J = 5.8 Hz, 2H), 2.06 (s, 9H), 1.65 (s, 6H); ^{13}C NMR (DMSO-d_6) δ 170.8, 147.3, 129.7, 124.4, 114.3, 51.1, 42.9, 41.5, 36.5, 29.3.

*N-(4-(2-((-Adamantan-1-yl)amino)-2-oxoethyl)phenyl)-4,6-difluoro-1H-indole-2-carboxamide (**23b**).* This compound was obtained *via* amide coupling 4,6-difluoroindole-2-carboxylic acid (**7**) and **22b** employing method A. The product was further crystallised from a 70% DCM/30% MeOH mixture and was obtained in >95% purity. White solid, yield: 96%.^{1}H NMR (DMSO-d_6) δ 12.15 (s, 1H), 10.24 (s, 1H), 7.68 (d, J = 8.6 Hz, 2H), 7.52 (s, 2H), 7.23 (d, J = 8.6 Hz, 2H), 7.07 (dd, J = 9.4, 1.4 Hz, 1H), 6.91 (td, J = 10.4, 2.1 Hz, 1H), 3.32 (s, 2H), 1.98 (s, 3H), 1.92 (s, 6H), 1.59 (s, 6H); ^{13}C NMR (DMSO-d_6) δ 170.0, 159.9 (dd, J = 239.0, 12.1 Hz), 159.3, 156.3 (dd, J = 249.0, 15.5 Hz), 138.4 (dd, J = 15.3, 13.0 Hz), 137.3, 133.0 (d, J = 3.2 Hz), 132.9, 129.6, 120.6, 113.6 (d, J = 21.9 Hz), 99.9, 95.9 (dd, J = 29.8, 23.2 Hz), 95.1 (dd, J = 25.9, 4.4 Hz), 51.2, 43.0, 41.4, 36.5, 29.3; HRMS (ESI) m/z calcd for $C_{27}H_{27}F_2N_3O_2$ ([M + H]$^+$) m/z 464.2144; found 464.2138.

6.2. Biological evaluation

6.2.1. Antitumour activity. The four well-established paediatric brain tumour cell lines were all derived from humans and were used to assess the effects on proliferation and viability when treated with the indole and indole bioisostere carboxamide derivatives. KNS42 (glioblastoma multiforme – GBM), BT-12 and BT-16 (atypical teratoid rhabdoid tumour – AT/RT) cell lines were gifts from Dr. Hashizume, Northwestern University, whereas DAOY cells (medulloblastoma – MB) were obtained from ATCC. The human fibroblasts HFF1 (obtained from ATCC) were used as non-neoplastic controls. The cells were cultured and the compounds were screened for their proliferation and viability inhibitory activities following the protocol described in our previous report.[38] Each experiment was executed in triplicate.

6.2.2. Transcriptional analysis of KNS42 cells. The KNS42 cells were maintained in Roswell Park Memorial Institute (RPMI) medium supplemented with 10% fetal bovine serum (FBS) and 1% penicillin/streptomycin and incubated at 37 °C in 5% CO_2. The cells were treated with 10 μM compound **8a**. The cells were washed with 1× PBS, scraped with a cell scraper and centrifuged to collect cell pellets after 72 hours of treatment. The RNA samples were then prepared according to our previous report[38] and were submitted to BGI Americas for DNBSEQ Eukaryotic Stranded Transcriptome Resequencing.

6.2.3. *In vitro* functional activity assay at CB_1R and CB_2R. Mouse AtT-20 neuroblastoma cells stably transfected with human CB_1R or human CB_2R were used for evaluation of membrane potential responses as previously reported.[82,83] In antagonist mode, cells were pre-incubated with the vehicle or compounds for 60 minutes, before addition of 500 nM CP 55940. Data were analysed with PRISM (GraphPad Software Inc., SanDiego, CA), using four-parameter non-linear regression to fit agonist (EC_{50}) and antagonist (IC_{50}) concentration response curves.

Conflicts of interest

There are no conflicts to declare.

Acknowledgements

SSRA acknowledges Curtin University for the support through a Curtin International Postgraduate Research Scholarship (CIPRS). HG is thankful for the ARC Discovery Early Career Researcher Award DE160100482.

References

1 F. He and Y. E. Sun, *Int. J. Biochem. Cell Biol.*, 2007, **39**, 661–665.
2 K. R. Jessen and R. Mirsky, *Nature*, 1980, **286**, 736–737.
3 Q. T. Ostrom, H. Gittleman, P. Liao, C. Rouse, Y. Chen, J. Dowling, Y. Wolinsky, C. Kruchko and J. Barnholtz-Sloan, *Neuro-Oncology*, 2014, **16**(Suppl 4), iv1–iv63.
4 D. N. Louis, A. Perry, G. Reifenberger, A. von Deimling, D. Figarella-Branger, W. K. Cavenee, H. Ohgaki, O. D. Wiestler, P. Kleihues and D. W. Ellison, *Acta Neuropathol.*, 2016, **131**, 803–820.
5 Z. Miklja, A. Pasternak, S. Stallard, T. Nicolaides, C. Kline-Nunnally, B. Cole, R. Beroukhim, P. Bandopadhayay, S. Chi, S. H. Ramkissoon, B. Mullan, A. K. Bruzek, A. Gauthier, T. Garcia, C. Atchison, B. Marini, M. Fouladi, D. W. Parsons, S. Leary, S. Mueller, K. L. Ligon and C. Koschmann, *Neuro-Oncology*, 2019, **21**(8), 968–980.
6 D. A. Bax, S. E. Little, N. Gaspar, L. Perryman, L. Marshall, M. Viana-Pereira, T. A. Jones, R. D. Williams, A. Grigoriadis, G. Vassal, P. Workman, D. Sheer, R. M. Reis, A. D. Pearson, D. Hargrave and C. Jones, *PLoS One*, 2009, **4**, e5209.
7 K. Ichimura, R. Nishikawa and M. Matsutani, *Neuro-Oncology*, 2012, **14**(Suppl 4), iv90–iv99.
8 C. Jones, L. Perryman and D. Hargrave, *Nat. Rev. Clin. Oncol.*, 2012, **9**, 400–413.
9 N. Gaspar, L. Marshall, L. Perryman, D. A. Bax, S. E. Little, M. Viana-Pereira, S. Y. Sharp, G. Vassal, A. D. Pearson, R. M. Reis, D. Hargrave, P. Workman and C. Jones, *Cancer Res.*, 2010, **70**, 9243–9252.
10 T. Mueller, A. S. G. Stucklin, A. Postlmayr, S. Metzger, N. Gerber, C. Kline, M. Grotzer, J. Nazarian and S. Mueller, *Curr. Treat. Options Neurol.*, 2020, **22**, 43.
11 M. Guzman, M. J. Duarte, C. Blazquez, J. Ravina, M. C. Rosa, I. Galve-Roperh, C. Sanchez, G. Velasco and L. Gonzalez-Feria, *Br. J. Cancer*, 2006, **95**, 197–203.
12 A. E. Munson, L. S. Harris, M. A. Friedman, W. L. Dewey and R. A. Carchman, *J. Natl. Cancer Inst.*, 1975, **55**, 597–602.
13 B. Chakravarti, J. Ravi and R. K. Ganju, *Oncotarget*, 2014, **5**, 5852–5872.
14 S. Sarfaraz, V. M. Adhami, D. N. Syed, F. Afaq and H. Mukhtar, *Cancer Res.*, 2008, **68**, 339–342.
15 P. Massi, M. Valenti, M. Solinas and D. Parolaro, *Cancers*, 2010, **2**, 1013–1026.
16 D. Parolaro and P. Massi, *Expert Rev. Neurother.*, 2008, **8**, 37–49.
17 F. C. Rocha, J. G. Dos Santos Junior, S. C. Stefano and D. X. da Silveira, *J. Neuro-Oncol.*, 2014, **116**, 11–24.
18 G. Velasco, A. Carracedo, C. Blazquez, M. Lorente, T. Aguado, A. Haro, C. Sanchez, I. Galve-Roperh and M. Guzman, *Mol. Neurobiol.*, 2007, **36**, 60–67.
19 G. Velasco, C. Sanchez and M. Guzman, *Nat. Rev. Cancer*, 2012, **12**, 436–444.
20 G. Velasco, C. Sanchez and M. Guzman, *Curr. Oncol.*, 2016, **23**, S23–S32.
21 M. Guzman, *Nat. Rev. Cancer*, 2003, **3**, 745–755.
22 C. Sanchez, I. Galve-Roperh, C. Canova, P. Brachet and M. Guzman, *FEBS Lett.*, 1998, **436**, 6–10.
23 C. Blazquez, L. Gonzalez-Feria, L. Alvarez, A. Haro, M. L. Casanova and M. Guzman, *Cancer Res.*, 2004, **64**, 5617–5623.
24 I. Galve-Roperh, C. Sanchez, M. L. Cortes, T. Gomez del Pulgar, M. Izquierdo and M. Guzman, *Nat. Med.*, 2000, **6**, 313–319.
25 A. Ellert-Miklaszewska, B. Kaminska and L. Konarska, *Cell. Signalling*, 2005, **17**, 25–37.
26 C. Blazquez, M. Salazar, A. Carracedo, M. Lorente, A. Egia, L. Gonzalez-Feria, A. Haro, G. Velasco and M. Guzman, *Cancer Res.*, 2008, **68**, 1945–1952.
27 R. Ramer and B. Hinz, *Int. Rev. Cell Mol. Biol.*, 2015, **314**, 43–116.
28 C. Blazquez, M. L. Casanova, A. Planas, T. Gomez Del Pulgar, C. Villanueva, M. J. Fernandez-Acenero, J. Aragones, J. W. Huffman, J. L. Jorcano and M. Guzman, *FASEB J.*, 2003, **17**, 529–531.
29 T. Gomez del Pulgar, G. Velasco, C. Sanchez, A. Haro and M. Guzman, *Biochem. J.*, 2002, **363**, 183–188.
30 C. Sanchez, M. L. de Ceballos, T. Gomez del Pulgar, D. Rueda, C. Corbacho, G. Velasco, I. Galve-Roperh, J. W. Huffman, S. Ramon y Cajal and M. Guzman, *Cancer Res.*, 2001, **61**, 5784–5789.
31 S. Fogli, P. Nieri, A. Chicca, B. Adinolfi, V. Mariotti, P. Iacopetti, M. C. Breschi and S. Pellegrini, *FEBS Lett.*, 2006, **580**, 1733–1739.
32 S. B. Gustafsson, T. Lindgren, M. Jonsson and S. O. Jacobsson, *Cancer Chemother. Pharmacol.*, 2009, **63**, 691–701.
33 P. Massi, A. Vaccani, S. Ceruti, A. Colombo, M. P. Abbracchio and D. Parolaro, *J. Pharmacol. Exp. Ther.*, 2004, **308**, 838–845.
34 P. Massi, A. Vaccani, S. Bianchessi, B. Costa, P. Macchi and D. Parolaro, *Cell. Mol. Life Sci.*, 2006, **63**, 2057–2066.
35 K. P. Sarker and I. Maruyama, *Cell. Mol. Life Sci.*, 2003, **60**, 1200–1208.
36 A. Vaccani, P. Massi, A. Colombo, T. Rubino and D. Parolaro, *Br. J. Pharmacol.*, 2005, **144**, 1032–1036.
37 Y. Shi, Y. H. Duan, Y. Y. Ji, Z. L. Wang, Y. R. Wu, H. Gunosewoyo, X. Y. Xie, J. Z. Chen, F. Yang, J. Li, J. Tang, X. Xie and L. F. Yu, *J. Med. Chem.*, 2017, **60**, 7067–7083.
38 S. S. R. Alsayed, S. Lun, A. W. Bailey, A. Suri, C.-C. Huang, M. Mocerino, A. Payne, S. T. Sredni, W. R. Bishai and H. Gunosewoyo, *RSC Adv.*, 2021, **11**, 15497–15511.
39 A. D. Rouillard, G. W. Gundersen, N. F. Fernandez, Z. Wang, C. D. Monteiro, M. G. McDermott and A. Ma'ayan, *Database*, 2016, **2016**, baw100.

40 S. P. Oldfield, M. D. Hall and J. A. Platts, *J. Med. Chem.*, 2007, **50**, 5227–5237.

41 C. Mugnaini, A. Brizzi, A. Ligresti, M. Allara, S. Lamponi, F. Vacondio, C. Silva, M. Mor, V. Di Marzo and F. Corelli, *J. Med. Chem.*, 2016, **59**, 1052–1067.

42 S. Pasquini, M. De Rosa, V. Pedani, C. Mugnaini, F. Guida, L. Luongo, M. De Chiaro, S. Maione, S. Dragoni, M. Frosini, A. Ligresti, V. Di Marzo and F. Corelli, *J. Med. Chem.*, 2011, **54**, 5444–5453.

43 S. Pasquini, A. Ligresti, C. Mugnaini, T. Semeraro, L. Cicione, M. De Rosa, F. Guida, L. Luongo, M. De Chiaro, M. G. Cascio, D. Bolognini, P. Marini, R. Pertwee, S. Maione, V. Di Marzo and F. Corelli, *J. Med. Chem.*, 2010, **53**, 5915–5928.

44 E. Stern, G. G. Muccioli, R. Millet, J. F. Goossens, A. Farce, P. Chavatte, J. H. Poupaert, D. M. Lambert, P. Depreux and J. P. Henichart, *J. Med. Chem.*, 2006, **49**, 70–79.

45 C. Manera, A. M. Malfitano, T. Parkkari, V. Lucchesi, S. Carpi, S. Fogli, S. Bertini, C. Laezza, A. Ligresti, G. Saccomanni, J. R. Savinainen, E. Ciaglia, S. Pisanti, P. Gazzerro, V. Di Marzo, P. Nieri, M. Macchia and M. Bifulco, *Eur. J. Med. Chem.*, 2015, **97**, 10–18.

46 S. S. R. Alsayed, S. Lun, G. Luna, C. C. Beh, A. D. Payne, N. Foster, W. R. Bishai and H. Gunosewoyo, *RSC Adv.*, 2020, **10**, 7523–7540.

47 P. Kancharla, J. X. Kelly and K. A. Reynolds, *J. Med. Chem.*, 2015, **58**, 7286–7309.

48 S. D. Banister, J. Stuart, R. C. Kevin, A. Edington, M. Longworth, S. M. Wilkinson, C. Beinat, A. S. Buchanan, D. E. Hibbs, M. Glass, M. Connor, I. S. McGregor and M. Kassiou, *ACS Chem. Neurosci.*, 2015, **6**, 1445–1458.

49 R. G. Pertwee, *Expert Opin. Invest. Drugs*, 2000, **9**, 1553–1571.

50 L. Ruiz, A. Miguel and I. Diaz-Laviada, *FEBS Lett.*, 1999, **458**, 400–404.

51 Y. Y. Ji, Z. L. Wang, F. N. Pei, J. J. Shi, J. J. Li, H. Gunosewoyo, F. Yang, J. Tang, X. Xie and L. F. Yu, *MedChemComm*, 2019, **10**, 2131–2139.

52 M. Koslowski, U. Sahin, R. Mitnacht-Kraus, G. Seitz, C. Huber and O. Tureci, *Cancer Res.*, 2007, **67**, 9528–9534.

53 C. Lin, P. Qian, Y. Zhang, Z. Liu, K. Dai and D. Sun, *Tissue Cell*, 2021, **69**, 101480.

54 Y. Wu, X. Lin, X. Di, Y. Chen, H. Zhao and X. Wang, *Oncol. Rep.*, 2017, **37**, 465–473.

55 C. Han, S. He, R. Wang, X. Gao, H. Wang, J. Qiao, X. Meng, Y. Li and L. Yu, *J. Transl. Med.*, 2021, **19**, 65.

56 T. Wang and M. Ha, *J. Cell. Biochem.*, 2018, **119**, 7747–7756.

57 W. Wang, T. Shen, B. Dong, C. J. Creighton, Y. Meng, W. Zhou, Q. Shi, H. Zhou, Y. Zhang, D. D. Moore and F. Yang, *J. Clin. Invest.*, 2019, **129**, 1015–1029.

58 T. Shen, W. Wang, W. Zhou, I. Coleman, Q. Cai, B. Dong, M. M. Ittmann, C. J. Creighton, Y. Bian, Y. Meng, D. R. Rowley, P. S. Nelson, D. D. Moore and F. Yang, *J. Clin. Invest.*, 2021, **131**(4), e135465.

59 D. Ganguly, C. Cai, M. M. Sims, C. H. Yang, M. Thomas, J. Cheng, A. G. Saad and L. M. Pfeffer, *Pharmaceuticals*, 2019, **12**(1), 45.

60 Z. Chen, X. Wei, X. Wang, X. Zheng, B. Chang, L. Shen, H. Zhu, M. Yang, S. Li and X. Zheng, *Cell Death Dis.*, 2021, **12**, 377.

61 Y. Yi, S. H. Tsai, J. C. Cheng, E. Y. Wang, M. S. Anglesio, D. R. Cochrane, M. Fuller, E. A. Gibb, W. Wei, D. G. Huntsman, A. Karsan and P. A. Hoodless, *Gynecol. Oncol.*, 2017, **147**, 663–671.

62 K. Kobayashi, A. Ohnishi, J. Promsuk, S. Shimizu, Y. Kanai, Y. Shiokawa and M. Nagane, *Neurosurgery*, 2008, **62**(2), 493–504.

63 Y. Ohshima, K. Kaira, A. Yamaguchi, N. Oriuchi, H. Tominaga, S. Nagamori, Y. Kanai, T. Yokobori, T. Miyazaki, T. Asao, Y. Tsushima, H. Kuwano and N. S. Ishioka, *Cancer Sci.*, 2016, **107**, 1499–1505.

64 Q. Wang, J. Tiffen, C. G. Bailey, M. L. Lehman, W. Ritchie, L. Fazli, C. Metierre, Y. J. Feng, E. Li, M. Gleave, G. Buchanan, C. C. Nelson, J. E. Rasko and J. Holst, *J. Natl. Cancer Inst.*, 2013, **105**, 1463–1473.

65 J. Wang, X. Chen, L. Su, P. Li, B. Liu and Z. Zhu, *Biomed. Pharmacother.*, 2013, **67**, 693–699.

66 Z. Haining, N. Kawai, K. Miyake, M. Okada, S. Okubo, X. Zhang, Z. Fei and T. Tamiya, *BMC Clin. Pathol.*, 2012, **12**, 4.

67 T. Nakayama, H. Hirakawa, K. Shibata, A. Nazneen, K. Abe, T. Nagayasu and T. Taguchi, *Oncol. Rep.*, 2011, **25**, 929–935.

68 Y. T. Tsai, A. C. Wu, W. B. Yang, T. J. Kao, J. Y. Chuang, W. C. Chang and T. I. Hsu, *Int. J. Mol. Sci.*, 2019, **20**(22), 5625.

69 Z. Wang, B. Han, Z. Zhang, J. Pan and H. Xia, *Biomarkers*, 2010, **15**, 39–46.

70 M. Cocchia, R. Huber, S. Pantano, E. Y. Chen, P. Ma, A. Forabosco, M. S. Ko and D. Schlessinger, *Genomics*, 2000, **68**, 305–312.

71 Y. Yin, X. Zhu, S. Huang, J. Zheng, M. Zhang, W. Kong, Q. Chen, Y. Zhang, X. Chen, K. Lin and X. Ouyang, *Tumor Biol.*, 2017, **39**, 1010428317699131.

72 H. Yuan, V. Chen, M. Boisvert, C. Isaacs and R. I. Glazer, *PLoS One*, 2018, **13**, e0192106.

73 J. Mahmoudian, R. Ghods, M. Nazari, M. Jeddi-Tehrani, M. H. Ghahremani, S. N. Ostad and A. H. Zarnani, *Exp. Oncol.*, 2019, **41**, 7–13.

74 B. K. Ang, C. Y. Lim, S. S. Koh, N. Sivakumar, S. Taib, K. B. Lim, S. Ahmed, G. Rajagopal and S. H. Ong, *J. Mol. Signaling*, 2007, **2**, 1.

75 Y. Katanasaka, Y. Kodera, Y. Kitamura, T. Morimoto, T. Tamura and F. Koizumi, *Mol. Cancer*, 2013, **12**, 31.

76 P. Kongpracha, S. Nagamori, P. Wiriyasermkul, Y. Tanaka, K. Kaneda, S. Okuda, R. Ohgaki and Y. Kanai, *J. Pharmacol. Sci.*, 2017, **133**, 96–102.

77 K. Oda, N. Hosoda, H. Endo, K. Saito, K. Tsujihara, M. Yamamura, T. Sakata, N. Anzai, M. F. Wempe, Y. Kanai and H. Endou, *Cancer Sci.*, 2010, **101**, 173–179.

78 L. La Paglia, A. Listi, S. Caruso, V. Amodeo, F. Passiglia, V. Bazan and D. Fanale, *PPAR Res.*, 2017, **2017**, 8187235.

79 A. Carracedo, M. Lorente, A. Egia, C. Blazquez, S. Garcia, V. Giroux, C. Malicet, R. Villuendas, M. Gironella, L. Gonzalez-Feria, M. A. Piris, J. L. Iovanna, M. Guzman and G. Velasco, *Cancer Cell*, 2006, **9**, 301–312.

80 S. S. R. Alsayed, S. Lun, A. Payne, W. R. Bishai and H. Gunosewoyo, *Bioorg. Chem.*, 2021, **106**, 104486.
81 K. Urgin, M. Jida, K. Ehrhardt, T. Muller, M. Lanzer, L. Maes, M. Elhabiri and E. Davioud-Charvet, *Molecules*, 2017, **22**, 161.
82 A. Knapman, M. Santiago, Y. P. Du, P. R. Bennallack, M. J. Christie and M. Connor, *J. Biomol. Screening*, 2013, **18**, 269–276.
83 M. Moir, S. Lane, F. Lai, M. Connor, D. E. Hibbs and M. Kassiou, *Eur. J. Med. Chem.*, 2019, **180**, 291–309.